



# Various Approaches to Reduce Consequences of Pedestrian–Tram Front End Collision

Roman JEŽDÍK<sup>1</sup>, Vladislav KEMKA<sup>2</sup>, Jan KOVANDA<sup>3</sup>, František LOPOT<sup>4</sup>, Hynek PURŠ<sup>5</sup>,  
Barbora HÁJKOVÁ<sup>6</sup>

Original Scientific Paper  
Submitted: 27 Sep. 2022  
Accepted: 1 Feb. 2023

<sup>1</sup> jezdik@vukv.cz, VÚKV a. s., Research, development and testing of railway rolling stock; Department of Anatomy and Biomechanics, Faculty of Physical Education and Sport, Charles University

<sup>2</sup> kemka@fst.zcu.cz, Regional Technology Institute, University of West Bohemia

<sup>3</sup> kovanda@fst.zcu.cz, Regional Technology Institute, University of West Bohemia

<sup>4</sup> lopot@ftvs.cuni.cz, Department of Anatomy and Biomechanics, Faculty of Physical Education and Sport, Charles University

<sup>5</sup> hpurs@advanced-eng.cz, Advanced Engineering, s.r.o.; Department of Anatomy and Biomechanics, Faculty of Physical Education and Sport, Charles University

<sup>6</sup> barbora.hajkova@skodagroup.cz, ŠKODA TRANSPORTATION a.s.; Department of Anatomy and Biomechanics, Faculty of Physical Education and Sport, Charles University



This work is licensed under a Creative Commons Attribution 4.0 International License

Publisher:  
Faculty of Transport and Traffic Sciences,  
University of Zagreb

## ABSTRACT

Safety of rail vehicles is an important feature of sustainable public transport. Proofs of an effort in that area are new recommendations and regulations from the expert commission (WG2 of the Technical Committee CEN / TC 256) regarding trams and light rail vehicles aimed at vulnerable road users. Additional requirements on tram safety can be requested by the vehicle operator and/or city. Pedestrian safety measures can be adopted from the automotive sector utilising the protection principles from Regulation EC No. 78/2009, ECE/UN regulations, and EuroNCAP tests. The purpose of this publication is to introduce a simplified testing method for the tram front end with respect to pedestrian head-on collisions. Testing methods based on segment impactors were generally accepted. The wrap-around distance defines the assessment of vehicle impact areas. A mathematical model was created to compare the results of the full-scale tests and the segment tests done by the standard and simplified aluminium head impactors. The tram front-end design can be tested using this alternate method, based on a simple impactor and easy methodology, providing an efficient tool to inspire both the tram manufacturers and vehicle operators to improve the vulnerable road users' safety in city traffic.

## KEYWORDS

passive safety; tram; head injury; pedestrian collision; tram safety; evaluation.

## 1. INTRODUCTION

As the density of urban traffic still increases, the problem of pedestrian safety in case of tram collision is a topic of interest from several points of view. The biomechanics of injuries is discussed in [1–3], and the influence of traffic organisation and logistics is mentioned in [4, 5]. The surface material evaluation is done in [6]. The problematics of vulnerable road users included e.g. cyclists, [7] is focused on their collision with a tram. The paper [8] provides a complex view of pedestrian crashes and uses the multibody simulation to define the vulnerability prediction tool for safety engineers.

A solution to the problem of pedestrian-tram collisions has been launched recently by the working group WG2 of the Technical Committee CEN / TC 256. The WG2 group prepared Technical Report TR 17420 “Railway Applications - Vehicle End Design for Trams and Light Rail Vehicles with Respect to Pedestrian Safety” [9]. It was issued in January 2020 and represents a base of a future European standard.

The technical report gives requirements on the structure of newly designed trams' front ends. The objectives are to provide protection for pedestrians by reducing the risk of severe injuries, being trapped under the

vehicle, being hit by underfloor equipment, and being run over by the wheels of the vehicle. Scenario A (collision with a standing pedestrian) and scenario B (collision with a lying pedestrian) are defined. Demonstration of requirements for scenario A can be performed in two ways. It is possible either to meet the geometric criteria on the front-end shape or perform a numerical simulation of pedestrian vs. tram front-end collision (pedestrian sideways to the tram), which demonstrates the meeting of required criteria, i.e. HIC criteria and deflection of a pedestrian from the tram track. The requirements for scenario B can be met only by a test with a lying mannequin. The mannequin differs from an anthropomorphic test device (=ATD, generally called a “crash test dummy”).

The above-mentioned numerical simulation assumes the use of a validated ATD simulation model. In order to obtain data for the validation of the ATD simulation model, a series of tests are carried out as part of the “Analysis of Pedestrian-Tram Accident Events – Validation of Simulation ATD Model” project. These are tests with an anthropomorphic test device in front and side positions colliding with the front surfaces of selected trams.

## 2. ATD APPROACH

As mentioned above the report [9] expects to use a validated model of standing ADT for side impact. The model can be validated against the behaviour of physical ADT only. Currently, there is only sitting ATD certified according to automotive regulations for side impact at the market, see [10] and *Figure 1*, left.



*Figure 1 – ATDs available [10]*

The certificated Hybrid-III 50th Percentile Male sitting ATD is typically used for front impact in automotive industry (see *Figure 1b*). This ATD can be modified using pedestrian kit parts to obtain standing ATD for front impact, but without certification (see *Figure 1c*). Use of the standing ATD for side impact is problematic as the impacting vehicle usually hits the shoulder. The shoulder design is a lug made of metal (see *Figure 2*). Its stiffness is unrealistic (too high). The transversal connection of the shoulders is also too stiff.



*Figure 2 – Shoulder articulation of ATDs*

## 2.1 Modelling

Both the ATD and the tram are considered as a continuum. It follows equation of motion (for the case of constant density), see [11], eq. (5.7.2):

$$\frac{\partial \tau_{ij}}{\partial x_j} + F_i = \rho \frac{\partial^2 u_i}{\partial t^2} \quad (1)$$

on volume  $\Omega$  where  $\tau_{ij}$  is stress tensor,  $F_i$  is volume force,  $\rho$  is constant density,  $u_i$  is displacement,  $x_i$  is coordinate and  $t$  is time. Relevant displacement and force boundary conditions:

$$u_i = f_i(x_j, t), \quad x_j \in \partial\Omega \quad (2)$$

$$T_i(x_j, t) = \tau_{ij} v_j, \quad x_j \in \partial\Omega \quad (3)$$

where  $\partial\Omega$  is surface of volume  $\Omega$ ,  $v_i$  is the surface normal vector,  $f_i$  is given displacement and  $T_i$  is given surface load at the surface  $\partial\Omega$ ; and relevant initial conditions:

$$u_i = f_i(x_j, t_0), \quad \frac{du_i}{dt} = g_i(x_j, t_0) \quad (4)$$

for initial time  $t_0$  need to be considered. The function  $g_i$  defines given initial velocity. The constitutive model is the relation:

$$\tau_{ij} = \tau_{ij} \left( \varepsilon_{ij}, \frac{d\varepsilon_{ij}}{dt} \right) \quad (5)$$

of stress tensor  $\tau_{ij}$  and strain tensor  $\varepsilon_{ij}$  which depends on displacement derivatives:

$$\varepsilon_{ij} = \varepsilon_{ij} \left( \frac{\partial u_k}{\partial x_l} \right). \quad (6)$$

The stress tensor in Equation 5 can be divided in a special case into elastic and plastic (dissipative) part. Considering 1D model, the elastic part is characterised by constant stiffness  $k$ , the plastic one by constant force  $F_{max}$  (see Figure 10).

The shape of modelled parts gives a volume  $\Omega$  on which the Equation 1 is solved. The stiffness and damping of model parts are adopted in constitutive models. Mass and inertia characteristics are reflected by density. Contact with the ground and mutual contacts between model parts give a nonzero force boundary condition. Initial positions and initial velocities of the model parts perform initial conditions (Equation 4) of Equation 1. Gravity is the only one nonzero external volume force  $F_i$ .

Solutions of equations of motion are performed by numerical methods, usually by finite element method with explicit time integration scheme. There are commercial implementations of this method (incl. ATD models) to be used, e.g. PAM-CRASH, LS-Dyna [12], Radios, etc.

## 2.2 Basic problems of validation of the ATD model

The complexity of the validation problem is demonstrated in this section. Besides the problem of not existing fully certified standing ATD, there are many practical problems to be solved. They are demonstrated when testing and modelling the collision of ATD with a tram. JASTI Hybrid III 50th Percentile Male Pedestrian ATD (see [10]) was used for testing. Numerical simulation was done using LSDyna. HYBRID III 50th Percentile Standing ADT model was used (see [13]).

### Positioning

The positioning of the ATD segment influences the time when individual segments come to contact with the tram structure. It defines the dynamic behavior of the entire ATD as the force pulses are shifted in time.

This phenomenon is illustrated by differences in longitudinal acceleration time histories of the head and pelvis, see Figure 3. The results of a real test of front collision and corresponding simulation with a mispositioned ATD model for collision speed 15 km/h are presented. The signals are shifted to achieve time coincidence of head acceleration peaks. As the time difference  $\Delta t$  is about 15 ms, the longitudinal misalignment is about  $d_M - d_T = 63$  mm.

Sensitivity on positioning of ATD hand during the side collision including comparing of test results will be published in a different paper of the project mentioned in acknowledgment.

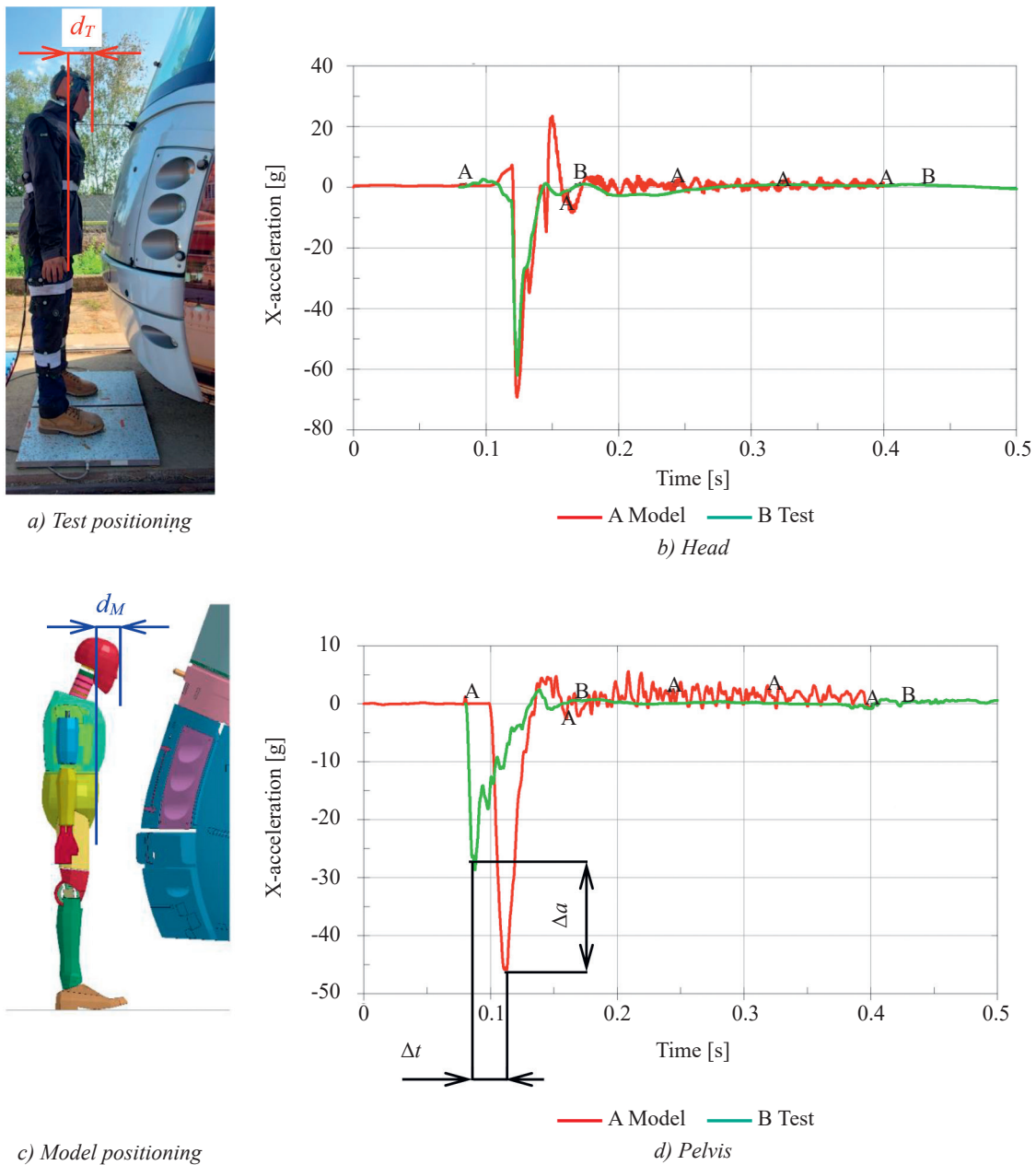


Figure 3 – Longitudinal acceleration time history – time difference due to different positioning of ATD

### Stiffness

The problem can be divided into the local stiffness of the ATD segment and the stiffness of the segment’s connection. It can be illustrated on a simple ADT model head shown in Figure 4. The head is represented by its centre of gravity (COG), mass and matrix of inertia. The local stiffness of the head as well as the stiffness of the neck is represented by equivalent springs.

Certain tests are required for certification in automotive industry. The local stiffness of the head is tested by the drop test. The stiffness/dumping of the real neck is tested by a pendulum test. As mentioned above, a standing ATD is derived from a sitting one using a pedestrian kid. The pedestrian kid consists of parts of the pelvis, lumbar spine and knee slider, which are not under certification. There are doubts about the local stiffness of thighs and pelvis when real ATD and ATD model are compared. The local stiffness of thighs is not so important for sitting ATD certification, and parts of pelvis of sitting ADT are replaced by the pedestrian kid. It is possible to see a difference ( $\Delta a \cong 18g$ ) when comparing pelvis acceleration peak of real ATD and ATD model (see Figure 3, bottom right).

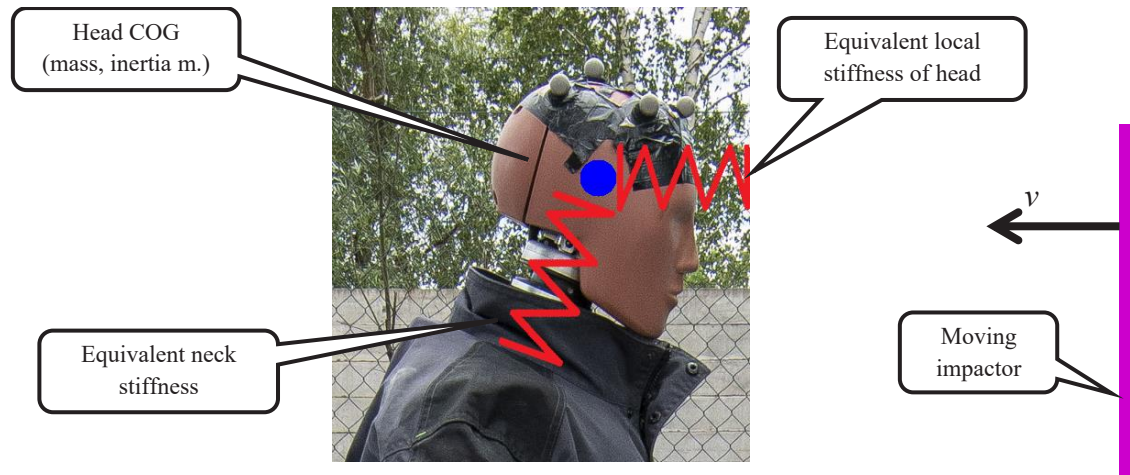


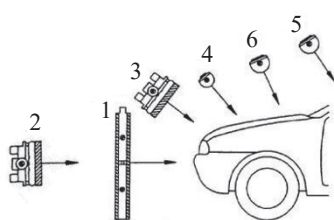
Figure 4 – Example of imaginary model of head-neck system of ATD

### 3. OTHER APPROACHES

The problems of ATD costs and ATD model validation mentioned above raise the question of the practical applicability of such a complex approach. A simpler and cheaper approach can be used to improve the current state of injury risk in urban traffic and increase the probability of its real application by manufacturers. The possibilities of such approaches are listed in this section.

#### 3.1 Automotive approach

Regulation No. 78/2009 [14] lists the conditions of type-approval of motor vehicles with regard to the protection of pedestrians and other vulnerable road users. There are prescribed tests using lower and upper legform and using child and adult head form, i.e. segment testing (see Figure 5).



- 1 – Lower legform to bumper test (Chapter II)
- 2 – Upper legform to bumper test (Chapter III)
- 3 – Upper legform to bonnet leading edge test (Chapter VI)
- 4 – Child/small adult headform to bonnet top test (Chapter V)
- 5 – Adult headform to windscreen test (Chapter VI)
- 6 – Child/small adult and adult headforms to bonnet top tests (Chapter VII)

Figure 5 – Segment testing of motor vehicles [14]

There are limits on the maximum knee bending angle, the maximum knee shear displacement and the upper end tibia acceleration not to be exceeded during lower legform testing. Upper legform testing limits are given by maximum force and maximum bending moment. Head acceleration tested by child and adult headform (see Figure 6) is limited by the head performance criterion (HPC). The headform impacts on both the car bonnet and windscreen. The impacted areas are divided to zones where HPC should not exceed the value 1,000 and areas where it should not exceed the value 2,000. This is due to the fact that there are always areas of higher stiffness on real car design.



Figure 6 – EC Adult 4.5 kg impactor: complete, skin and skull [10]

### 3.2 Adoption of automotive approach for trams and LRV

As the [9] prescribes only the limit on HIC criterion, this adoption is focused on head injury only.

#### Head injuries and injury criterion

Despite the significant progress in passive vehicle safety development over the past years aimed at reducing the number and extent of head injuries, there is a relatively narrow set of criteria for assessing the extent of injuries in vehicle and pedestrian crash tests [15]. These criteria are based only on monitoring the acceleration response. In other words, they do not take into account the assessment of the degree of injury caused by damage to the bone structures of the skull. The only anthropometric device capable of measuring force responses in the facial area is a THOR-type test dummy, which, however, is not included in the latest crash test standards.

Many post-mortem head injury studies have been conducted to investigate the mechanical properties of the head response. In general, impact reactions have been described in terms of acceleration and impact force, and therefore on the inertia of the head and the size of the impact surface. The average head weight of 50% man is  $m = 4.54 \text{ kg}$  and the average moments of inertia are  $I_{xx} = 0.022 \text{ kg} \cdot \text{m}^2$ ,  $I_{yy} = 0.0242 \text{ kg} \cdot \text{m}^2$ ,  $I_{zz} = 0.0159 \text{ kg} \cdot \text{m}^2$ .

In the performed studies, the impact tests were described mainly on a solid and flat surface. However, a major problem arose in their implementation; it was not possible to install the accelerometer in the centre of gravity of the head.

Extensive head acceleration tests resulted in the derivation of the Wayne State University Cerebral Concussion Tolerance Curve (WSTC, see Figure 7), which expresses the relationship between duration and the average magnitude of the anteroposterior translational acceleration. The combination of the magnitude of the acceleration and the time of its action occurring in the area above the curve presupposes exceeding the degree of tolerance, i.e. it causes serious, irreversible brain damage. The combination of these quantities acting in the area under the curve does not exceed the imaginary level of tolerance, but may result in a reversible injury. The original WSTC only covered the duration of the load until 6 ms, after which the curve was extended using animal measurements and volunteers.

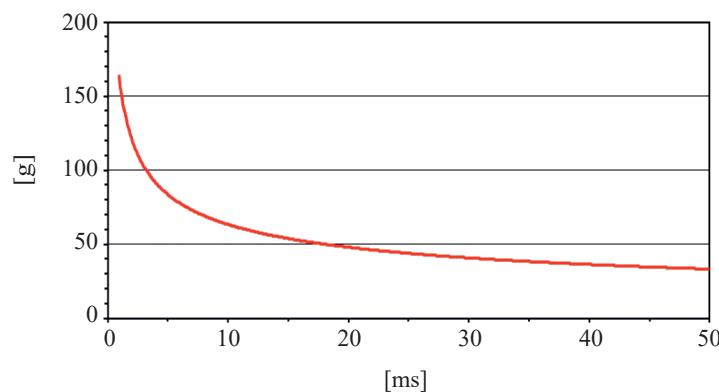


Figure 7 – WSTC – Wayne State Tolerance Curve [17]

The *Head Performance Criterion (HPC)* is the most commonly used criterion for assessing head injuries in vehicle crash tests. The input data for the calculation are the course of acceleration measured by accelerometers, which are located in the centre of gravity of the head of the test dummy. The value of the criterion is then determined from the given time interval of the course of the total acceleration. The interval range is set to 36 ms (HPC36) in the event without hard head contact during the impact. For hard head contact, the interval range is 15 ms (HPC15). The interval range of 15 ms is considered for pedestrian impacts because they usually correspond to a hard contact case. The resulting value of HPC should not exceed 1,000 in vehicle crashes and in specified areas of vehicle surface in the case of pedestrian crashes [15].

$$HPC = \left\{ (t_2 - t_1) \left[ \frac{1}{(t_2 - t_1)} \int_{t_1}^{t_2} a(t) dt \right]^{2.5} \right\}_{max} \quad (7)$$

$$a = \sqrt{a_x^2 + a_y^2 + a_z^2} \tag{8}$$

where:  $a$  is resulting acceleration [g],  $t_1$  is beginning of time interval [s] and  $t_2$  is end of time interval [s].

The resulting time interval is defined by the maximum of the formula, where the nominator is the integral of the acceleration signal in the power of 2.5, the denominator is the time interval  $\Delta t = t_2 - t_1 < 15$  ms in the power of 1.5.

The HPC criterion value is in principle identical to the head injury criterion (HIC) value, which is used still frequently in practice. The HIC criterion is used in this text.

The *Generalized Acceleration Model for Brain Injury Threshold (GAMBIT)* is an injury criterion that considers both the displacement and the rotation of the head during a vehicle impact. The maximum allowable value of the GAMBIT criterion ( $t \leq 1$ ).

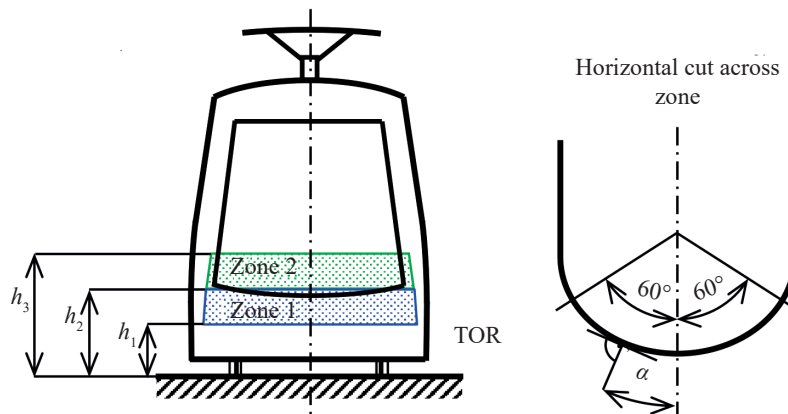
$$GAMBI(t) = \left[ \left( \frac{a}{a_{max}} \right)^m + \left( \frac{\omega}{\omega_{max}} \right)^n \right]^{\frac{1}{s}} \tag{9}$$

where:  $a$  is longitudinal acceleration [m·s<sup>-2</sup>],  $\omega$  is angular acceleration [rad·s<sup>-2</sup>] and  $g$  gravity acceleration ( $1 g = 9,81 \text{ m·s}^{-2}$ ). Limit values can be defined as:  $a_{max} = 250 g$ ,  $\omega_{max} = 10,000 \text{ rad·s}^{-2}$  and  $s = m = n = 1$ .

The measured data processing is described in the relevant literature. The GAMBIT criterion provides more complex process evaluation, however HIC (resp. HPC) has a long history in passive safety, and in spite of its drawbacks it is a leading head protection criterion [18]. It considers the diffuse brain injury mechanisms which are based on the elastic wave propagation through the tissue [19].

*Boundaries of zones under consideration*

As the shape of tested vehicles and typical collision velocities differ in automotive and tram or light rail vehicle (LRV) traffic, the risk injury evaluation is to be modified. It is supposed that the angle of the tram front end surface normal related to the horizontal direction is typically small. The two zones are purposed to define areas to be checked from the point of view of head injury, see *Figure 8*.



Zone	Boundary	Impactor	Criterion
1	$h_1 = 1.0 \text{ m}$	Iso Child 3.5 kg	HIC < 1,000 on 70% of zone area
	$h_2 = 1.5 \text{ m}$		HIC < 2,000 on 25% of zone area
	$\alpha \leq 60^\circ$		not evaluated on 5% of zone area*
2	$h_2 = 1.5 \text{ m}$	Iso Adult 4.5 kg	HIC < 1,000 on 70% of zone area
	$h_3 = 2.0 \text{ m}$		HIC < 2,000 on 25% of zone area
	$\alpha \leq 60^\circ$		not evaluated on 5% of zone area*

\* As the real design has to contain parts to be installed (e.g. lights, windscreen wipers, etc.), 5% of zone area is excluded from evaluation

Figure 8 – Evaluated areas of tram/LRV and limits

The lower edge level of zone 1 (1,000 mm above TOR) is based on the height of the 6-year-old child. The upper edge level of zone 2 (2,000 mm above TOR) is than based on the height of 95th percentile adult. The boundary between zones is considered at level of 1,500 mm above TOR as a typical height on changeover from child to adult. The wrap around measure is used to define zones in the automotive industry. It could be alternatively used in LRV industry. But a typical shape of LRV gives small differences between zone heights defined by wrap around method and the constant ones.

The width of zones is limited by the relation:

$$\alpha \leq 60^\circ \quad (10)$$

where angle  $\alpha$  is angle between projection of surface normal to horizontal plane and longitudinal direction (see *Figure 8*).

### *Impactor and criterions*

The automotive head form (adult for zone 1 and child for zone 2 [14]) is used instead of an entire dummy. Suggestions of limit values of the HIC criteria are proposed (see *Figure 8*) while taking into account the requirements of [9], the automotive approach and the possibility of practical realisation. As the real tram frontend design has to contain parts to be installed (e.g. lights, windscreen wipers etc.), 5% of zone area is excluded from evaluation.

### *Impact velocity and its direction*

The scenario A described in [9] is taken as a base. The real impact velocity vector will probably only slightly deviate from the horizontal plane.

Impactor initial velocity can be generated using the following basic mechanisms: drop mechanism, catapult mechanism, pendulum mechanism.

The drop mechanism is convenient for parts that can be placed under it. As testing of the complete tram front end is assumed, use of a drop mechanism is practically impossible.

The catapult mechanism is usually engaged to generate the initial velocity of the headform impactor used for testing in the automotive industry. The catapult mechanism is a stationary device, and the tested car is transported and positioned under it. This approach is not practical to use in the railway industry, as well as the use of a mobile catapult.

The pendulum mechanism appears to be the easiest way to generate initial velocity. Two types of suspension can be used to provide stable movement of the impactor for real LRV front end testing: suspension on one beam, double string suspension.

Suspension on one beam influences the behaviour of the impactor due to its own stiffness and its own inertia properties. For instance, when a structure with a significant angle  $\alpha$  is tested, the lateral movement of the impactor is significantly influenced by the suspension beam. Double string suspension looks like a good compromise between practicability and level of undesirable influence on the impactor. However, it is necessary to take into account one disadvantage. It is the fact that for bigger angle  $\alpha$  values it is not possible to perform the test when impact velocity vector is parallel to driving direction. The reason is the risk of the contact of the suspension string with the tested front end. To avoid the risk, the impact velocity vector is considered as the opposite one to the horizontal projection of the surface normal.

### **3.3 Automotive approach with simplified impactor**

The previous approach assumes using two headform impactors. It can be quite an expensive approach from the point of view of small series manufacturing. The simplified impactor shape with the contact sphere made of aluminium alloy is proposed, see *Figure 9*. As the spherical surface radius  $R$  is the same for the adult and child headforms (see [14]), only one impactor with removable masses can be used to have the required impactor mass while the impactor centre of gravity is kept in the centre of the spherical surface. The influence of using simplified AL impactors on the resulting HIC15 value was investigated by means of following case when the impactor hits a structure with initial velocity  $v_0 = 20$  km/h. The structure has a pure elasto-plastic loading characteristic (stiffness  $k$  and maximum force  $F_{max}$ ), and unloading follows a line characterised by stiffness  $k$ . The case is schematically shown in *Figure 10*.

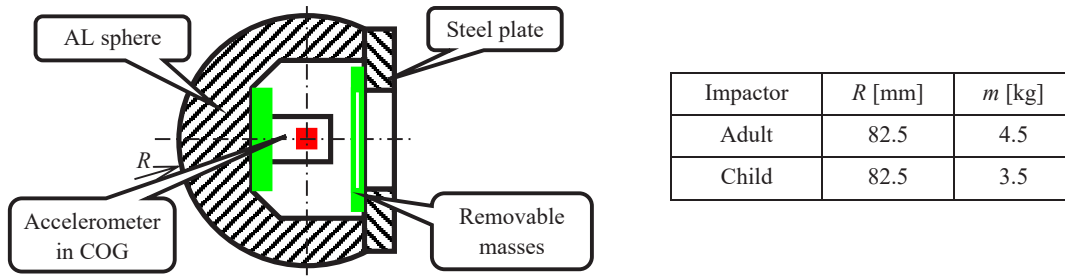


Figure 9 – Simplified AL impactor shape

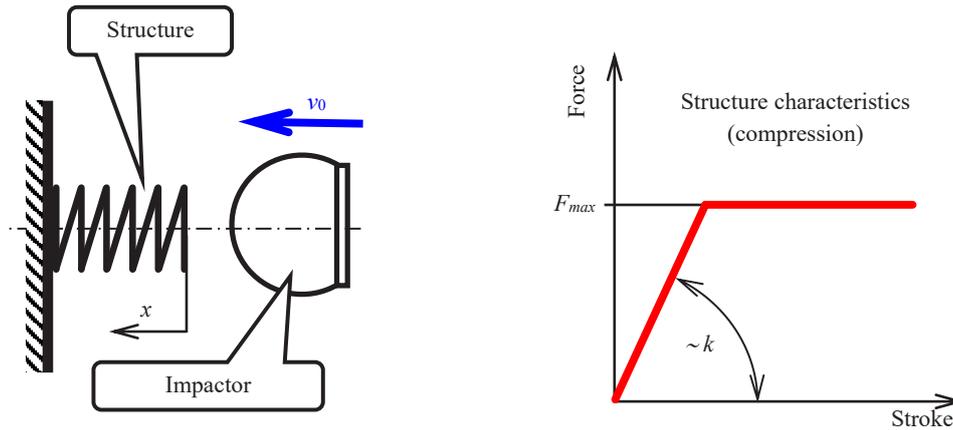


Figure 10 – Impact on pure elasto-plastic structure

The behaviour of the system is described by the following equation:

$$m\ddot{x} = F(x) \tag{11}$$

where  $m$  is the impactor mass,  $x$  is the impactor position, and  $\ddot{x}$  is its acceleration. If the impactor position is measured from spring free surface, then the force in loading phase is given as:

$$F(x) \begin{cases} 0 & x < 0, \\ -kx, & x \geq 0, \quad kx \leq F_{max} \\ -F_{max}, & x \geq 0, \quad kx > F_{max} \end{cases}$$

The force in unloading phase is given by the relation:

$$F(x) \begin{cases} 0 & x < x_p \\ -k(x - x_p), & x \geq x_p \end{cases}$$

where  $x_p$  is the plastic stroke of the spring.

The investigation was done for both an adult impactor of 4.5 kg and a child impactor of 3.5 kg. The structure stiffness  $k$  was considered to be between  $10^2$  N/mm and  $10^4$  N/mm. The maximum force value  $F_{max}$  was based on the assumption of a constant acceleration  $A$ . The impactor is stopped by the constant acceleration from the initial velocity  $v_0$  during the time interval  $\Delta T$ :

$$\Delta T = \frac{v_0}{A} \tag{12}$$

Considering Equation 7, we obtain the value of the constant acceleration:

$$A = \left[ \frac{HIC \cdot g^{2.5}}{v_0} \right]^{\frac{2}{3}} \tag{13}$$

where  $g = 9.81 \text{ m/s}^2$  gravitational acceleration which occurs in this relation as the acceleration in Equation 7 has to be considered in units of  $g$ . Considering the limit value of the criterion  $HIC_{15} = 1,000$  (commonly accepted limit see [14–16]), we obtained the value of the constant acceleration  $A = 146g$ . The corresponding maximum

force values  $F_{max}$  for adult impactor is 6,449 N, and for child impactor 5,016 N.

Three solutions were performed: analytical solution with a rigid body, numerical simulation with an AL impactor, numerical simulation with a headform.

The LS-DYNA solver by LSTC Company and its headform models were used to perform numerical simulations. The space discretisation was done using the finite element method, the time discretization by means of an explicit integration scheme. The headform models were modified to simulate an AL impactor. All parts of these models were modelled as rigid body, but the contact area had the properties of aluminium alloy.

*Analytical solution*

The analytical solution has to be divided to two cases: pure elastic case and elastic-plastic case.

Pure elastic case is the case when  $kx \leq F_{max}$  and  $x_p = 0$ . Loading and unloading phase for  $x \geq 0$  is characterized by force  $F(x) = -kx$ . The force  $F(x) = 0$  for negative  $x$ . Considering initial conditions

$$t = 0, \quad x_{(0)} = 0, \quad \dot{x}_{(0)} = v_0 \tag{14}$$

where  $t$  denotes time, the solution of Equation 11 has to be divided to two phases. The first one is the phase of impactor contact with the structure ( $t \leq T$ ):

$$x_{(t)} = \frac{v_0}{\omega} \sin(\omega t), \quad t \leq T \tag{15}$$

where:  $\omega = \sqrt{\frac{k}{m}}$  is eigen frequency, and  $T = \frac{\pi}{\omega}$  is a period which corresponds to time when impactor loses contact with the structure. The corresponding velocity and acceleration then are:

$$\dot{x}_{(t)} = v_0 \cos(\omega t), \quad t \leq T \tag{16}$$

$$\ddot{x}_{(t)} = -v_0 \omega \sin(\omega t), \quad t \leq T. \tag{17}$$

The second one is the phase when the impactor moves away ( $t > T$ ):

$$x_{(t)} = -v_0 t, \quad t > T. \tag{18}$$

The corresponding velocity and acceleration then are:

$$\dot{x}_{(t)} = v, \quad t > T \tag{19}$$

$$\ddot{u}_{(t)} = 0, \quad t > T \tag{20}$$

The stiffness  $\bar{k}$  when  $F_{u} = \bar{k} \frac{v_0}{\omega}$  is the border between pure elastic case and elastic-plastic case. It gives:

$$\bar{k} = \frac{1}{m} \left( \frac{F_{max}}{v_0} \right)^2 \tag{21}$$

An elastic-plastic case is the case when  $kx > F_{max}$ . The solution of Equation 11 has to be divided to four phases: elastic loading, plastic loading, elastic unloading and moving away.

The initial conditions of the *elastic loading phase* are the same as in case of the pure elastic case (see Equation 14). The solution is also the same (see Equation 15), but the end time of this phase corresponds to the moment  $T_1$  when the compression force reaches the value  $F_{max}$ . If a constant acceleration  $A = F_{max}/m$  is defined, then:

$$\ddot{x}_{(T_1)} = -A \tag{22}$$

Using Equation 17 we obtain:

$$-v_0 \omega \sin(\omega T_1) = -A \tag{23}$$

therefore:

$$T_1 = \frac{1}{\omega} \arcsin \left( \frac{A}{v_0 \omega} \right) \tag{24}$$

Considering Equation 15 the impactor position in time  $T_1$  is given as:

$$\ddot{u}_1 \approx_{(T_1)} \frac{v_0}{\omega} \sin(\omega T_1) - \frac{A}{\omega^2} \tag{25}$$

and the velocity in the same time then is:

$$v_1 = \dot{x}_{(T_1)} = v_0 \cos(\omega T_1) = v_0 \left[ 1 - \left( \frac{A}{v_0 \omega} \right)^2 \right]^{\frac{1}{2}} \tag{26}$$

The structure reaction to the impact in the *plastic loading phase* is characterised by the constant force value  $F_{max}$  and constant acceleration  $A$ , respectively. The initial conditions for this phase are given by the conditions at the end of the previous phase, see Equations 25 and 26. The solution of the Equation 11 for constant right side  $F(x) = -F_{max}$  gives a relation for impactor position in this phase:

$$x_{(t)} = x_1 + (v_1 + AT_1)(t - T_1) - \frac{1}{2} A(t^2 - T_1^2), \quad T_1 < t \leq T_2 \tag{27}$$

The corresponding velocity and acceleration are

$$\dot{x}_{(t)} = v_1 - A(t - T_1), \quad T_1 < t \leq T_2 \tag{28}$$

$$\ddot{x}_{(t)} = -A, \quad T_1 < t \leq T_2 \tag{29}$$

where the end time  $T_2$  of this phase comes when the impactor is stopped, i.e.  $v_2 = \dot{x}_{(T_2)} = 0$ . It gives:

$$T_2 = T_1 + \frac{v_1}{A} \tag{30}$$

The position of the impactor at the end of this phase is:

$$x_2 = x_{(T_2)} = x_1 + (v_1 + AT_1)(T_2 - T_1) - \frac{1}{2} A(T_2^2 - T_1^2) \tag{31}$$

In the *elastic unloading phase* the structure accelerates the impactor away after it is stopped. Initial conditions for this phase are given by the conditions at the end of the previous phase again. The initial level of the force  $F_{max}$ , the initial impactor position  $x_2$  and velocity  $v_2$  must be considered when solving Equation 11 in this phase. It gives:

$$x_{(t)} = x_2 - \frac{A}{\omega^2} \{1 - \cos[\omega(t - T_2)]\}, \quad T_2 < t \leq T_3 \tag{32}$$

The corresponding velocity and acceleration are

$$\dot{x}_{(t)} = -\frac{A}{\omega} \sin[\omega(t - T_2)], \quad T_2 < t \leq T_3 \tag{33}$$

$$\ddot{x}_{(t)} = -A \cos[\omega(t - T_2)], \quad T_2 < t \leq T_3 \tag{34}$$

where the end time  $T_3$  of this phase comes when the structure stops accelerating of the impactor, i.e.  $\ddot{x}_{(T_3)} = 0$ . It gives:

$$T_3 = T_2 + \frac{\pi}{2\omega} \tag{35}$$

### Results

The accelerations obtained by the above presented analytical solution and by the numerical simulations for AL impactors and headforms were processed to obtain the corresponding HIC15 criterion depending on structure stiffness  $k$ . The values 100, 125, 150, 175, 200, 233, 250, 275, 300, 325, 350, 375, 400, 500, 800, 1,000, 1,500 and 10,000 N/mm were considered. It should be noted that the stiffness values  $\bar{k} = 300$  N/mm and 233 N/mm, respectively, are on the border of pure elastic and elastic-plastic cases, see Equation 21.

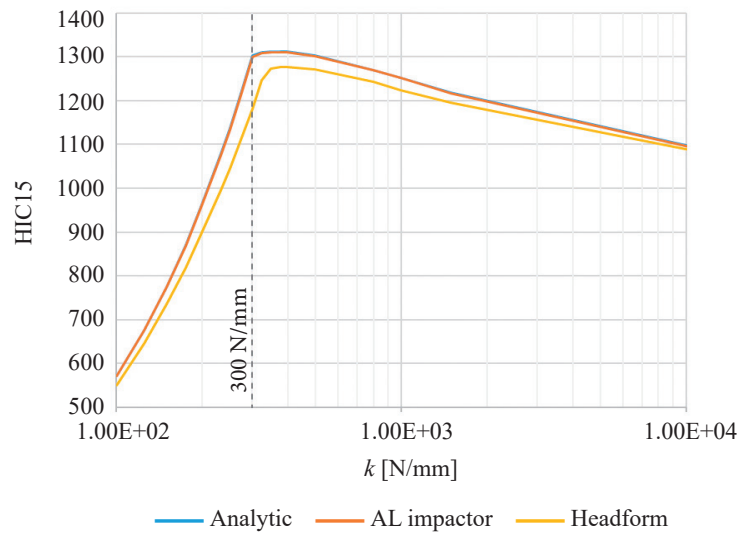


Figure 11 – HIC15 criterion for adult impactors

The results are shown in *Figure 11* for the case of adult impactor and in *Figure 12* for the case of child impactor. Considering the HIC15 criterion, the analytical results and simulation results for AL impactors are practically identical. The stiffness of the headform impactor is lower than that of the AL impactor, because the headform impactor is equipped by a flexible skin part. Due to this additional flexibility, the acceleration and HIC15 values of the headform impactors are smaller than the accelerations of AL impactors. The ratio of HIC15 obtained for the AL impactor and headform impactor is shown in *Figure 13*. The ratio is greater than one, i.e. AL impactors give for all stiffness samples under consideration higher values of HIC15 than the headform impactors do. The maximum observed difference is 10% and 8%, respectively for the adult and child impactor. It occurs for the stiffness  $\bar{k}$  on the border of a pure elastic and elastic-plastic case.

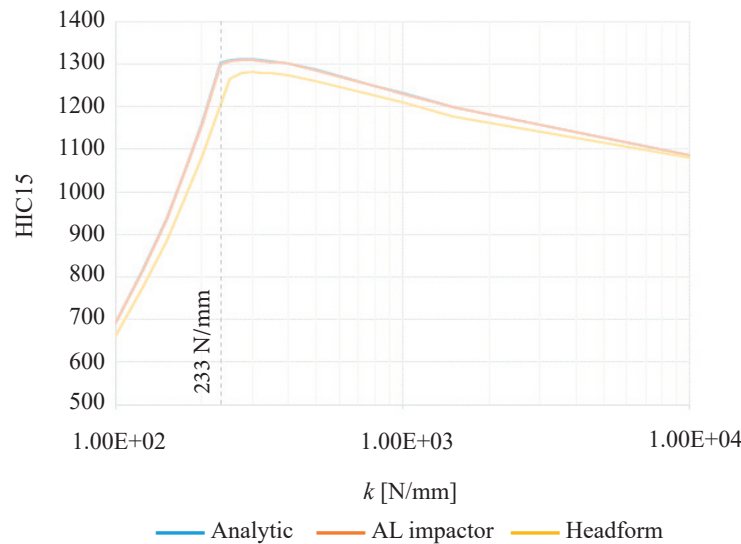


Figure 12 – HIC15 criterion for child impactors

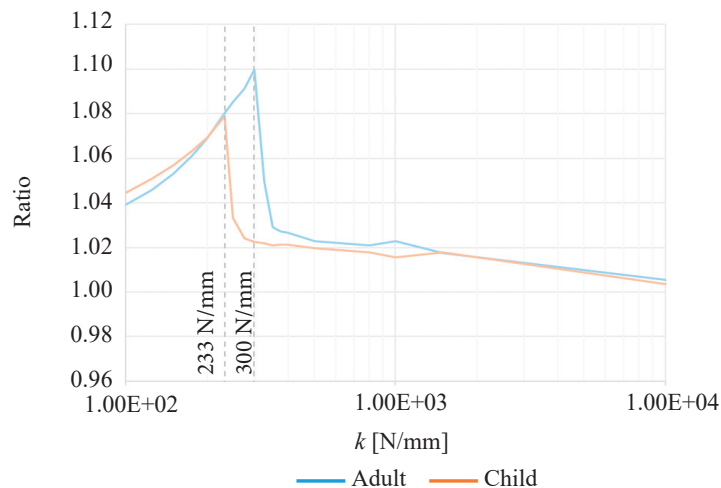


Figure 13 – HIC15 by AL and headform impactor ratio

#### 4. CONCLUSION

The approach expecting evaluation by ATD used in the report [9] was applied to selected trams. This approach seems to be very complicated and expensive in terms of practical use. However, the report [9] is the base document for the creation of a future European standard. The conclusions of the presented research will be presented to WG2 of the Technical Committee CEN / TC 256 as the argument for the development of new regulations. The method utilises both real and virtual testing approach.

Similar issues are solved by segmental testing (adult and child headform, upper leg and lower leg) in the automotive industry. Attention has been paid to the HIC criterion because the report [9] focuses only on it. A proposal to adopt the automotive approach (testing via headforms) for tram vehicles is presented. Boundaries of the evaluated tram front-end areas, including the suggestion of limit values of the HIC criteria, were proposed while taking into account the requirements of [9], the automotive approach and the possibility of practical realisation.

Furthermore, a simplification has been proposed in terms of the use of an AL impactor instead of a headform. The differences in the resulting HIC values for the headform and the AL impactor were investigated using numerical simulations. A model of a pure elasto-plastic structure was considered. An analytical solution was used to verify results. It was found that the results of the analytical solution and the AL impactor correspond to each other. The resulting HIC values are lower when using the headform than when using the AL impactor. The use of the AL impactor instead of the headform is on the safety side. The biggest differences occur at the interface of elastic and plastic behaviour of the structure. It is 10% for the adult headform and 8% for the child headform.

The approach proposed aims to simplify its practical application, while keeping the chosen level of passive safety. The simplification of the approach aims to increase the probability of its practical application. A mobile aluminium scaffolding, the AL impactor suspended on two steel ropes and a three-axial accelerometer with a measuring computer are sufficient to perform the test.

The simplification presented does not take into account possible differences due to local effects, the fact that the surface stiffness of the AL impactor itself is greater than the surface stiffness of the headform itself. This can lead to some differences in cases where local failure of the vehicle structure at the point of contact with the impactor occur during the impact. AL impactor use is convenient for structures evincing behaviour similar to the pure elastic-plastic one. That could include ductile metals or some sandwich materials (fiber glass laminated skins with polyurethane foam core). The possibility of using of the AL impactor instead of the headform is an open point of discussion.

## ACKNOWLEDGMENT

The project was funded by Operational Programme Research, Development and Education CZ.02.1.01/0.0/0.0/16\_026/0008401.

## REFERENCES

- [1] Stanton NA. *Advances in human aspects of transportation, Proceedings of the AHFE 2021 Virtual Conference on Human Aspects of Transportation, 25-29 July 2021, USA*. 2021. DOI: 10.1007/978-3-030-80012-3.
- [2] Chen P-L, Jou R-C, Saleh W, Pai C-W. Accidents involving pedestrians with their backs to traffic or facing traffic: An evaluation of crash characteristics and injuries. *Journal of Advanced Transportation*. 2016;50(5). DOI: 10.1002/atr.1372.
- [3] Arregui-Dalmases C, et al. *Pedestrian protection overview*. Encyclopedia of automotive engineering. 2014.
- [4] Naznin F, Curie G, Sarvi M. Safety impacts of platform tram stops on pedestrians in mixed traffic operation: A comparison group before–after crash study. *Accident Analysis & Prevention*. 2016;86:1-8. DOI: 10.1016/j.aap.2015.10.007.
- [5] Nasri M, Aghabayk K, Esmaili A, Shiwakoti N. Using ordered and unordered logistic regressions to investigate risk factors associated with pedestrian crash injury severity in Victoria, Australia. *Journal of Safety Research*. 2022;81:78-90. DOI: 10.1016/j.jsr.2022.01.008.
- [6] Shivakumar K, Deb A, Chou C. An exploration of jute-polyester composite for vehicle head impact safety countermeasures. *SAE International Journal of Materials and Manufacturing USA*. 2018;11(4). DOI: 10.4271/2018-01-0844.
- [7] Teschke K, et al. Bicycling crashes on streetcar (tram) or train tracks: Mixed methods to identify prevention measures. *BMC Public Health*. 2016;16:617. DOI: 10.1186/s12889-016-3242-3.
- [8] D'Apuzzo M, et al. Towards a better understanding of vulnerability in pedestrian-vehicle collision. *International Conference on Computational Science and Its Applications – ICCSA 2021*. Springer Nature Switzerland AG; 2021. p. 557-572. DOI: 10.1007/978-3-030-87016-4\_40.
- [9] TR 17420. *Railway applications - Vehicle end design for trams and light rail vehicles with respect to pedestrian safety*. Technical Committee CEN/TC 256; 2020.
- [10] JASTI CO. LTD. *Anthropomorphic test devices Dummy*. <https://www.jasti.co.jp/en/product/dummy.html#pedestrian> [Accessed 9<sup>th</sup> June 2021].
- [11] Brdička M, Samek L, Sopko B. *Continuum mechanics [Mechanika kontinua]*. Prague: Academia; 2005.
- [12] Ansys. LS-Dyna – Multiphysics Solver. <http://lsc.com/products/ls-dyna> [Accessed 9<sup>th</sup> June 2021].
- [13] [https://www.lsc.com/download/dummy\\_models](https://www.lsc.com/download/dummy_models)
- [14] EUR-Lex. *Regulation (EC) No 78/2009 of the European parliament and of the council of 14 January 2009 on the type-approval of motor vehicles with regard to the protection of pedestrians and other vulnerable road users, amending Directive 2007/46/EC and repealing Directives 2003/102/EC and 2005/66/EC*. <https://eur-lex.europa.eu/legal-content/EN/ALL/?uri=CELEX:32009R0078>.
- [15] *Crash analysis criteria description, Version 2.1.1*. Workgroup Data Processing Vehicle Safety. 2008. <https://vdocument.in/crash-analysis-criteria-arbeitskreis-messdatenverarbeitung-fahrzeugsicherheit-crash.html?page=1>.
- [16] United Nations Economic Commission for Europe (United Nations Economic and Social Council). *Regulation No 94 of the Economic Commission for Europe of the United Nations (UN/ECE) — Uniform provisions concerning the approval of vehicles with regard to the protection of the occupants in the event of a frontal collision*. OJ L 254 20.09.2012. p. 77. <http://data.europa.eu/eli/reg/2012/94/oj>.
- [17] Wismans J, et al. *Injury biomechanics*. Eindhoven University of Technology; 1994.
- [18] Namjoshi DR, et al. Towards clinical management of traumatic brain injury: A review of models and mechanisms from a biomechanical perspective. *Dis Model Mech*. 2013 Nov;6(6):1325-38. DOI: 10.1242/dmm.011320.
- [19] Hozman J, Bradáč J, Kovanda J. Neural tissue response to impact – Numerical study of wave propagation at level of neural cells. *Neural Network World*. 2014;24(2):157-176. DOI: 10.14311/NNW.2014.24.010.

Roman Ježdík, Vladislav Kemka, Jan Kovanda, František Lopot, Hynek Purš, Barbora Hájková

### Různé přístupy ke snižování následků kolize chodce s čelem tramvaje

#### Abstrakt

Bezpečnost kolejových vozidel je důležitou součástí udržitelné veřejné dopravy. Důkazem této snahy jsou nová doporučení a předpisy odborné komise (WG2 Technické komise

CEN / TC 256) týkající se tramvají a lehkých kolejových vozidel se zaměřením na zranitelné účastníky dopravy. Další požadavky na bezpečnost tramvají si může vyžádat provozovatel vozidla a/nebo město. Opatření pro bezpečnost chodců mohou být převzata z oblasti automobilů využitím principů z předpisů EU č. 78/2009, EHK/OSN a testů EuroNCAP. Cílem publikace je představit zjednodušenou zkušební metodiku pro čelo tramvaje s ohledem na bezpečnost chodců, kde byla přijata metoda testování pomocí impaktorů. Oblasti nárazu byly definovány obvodovými vzdálenostmi na svislém řezu karosérie. Matematický model byl vytvořen pro porovnání výsledků testů s figurínou, standardními a zjednodušenými hliníkovými impaktory. Uvedená metodika umožňuje testovat přední část tramvaje alternativní metodikou založenou na jednoduchém impaktoru a poskytuje účinný nástroj, který může výrobce a provozovatele tramvají inspirovat ke zvýšení bezpečnosti zranitelných účastníků dopravy.

**Klíčová slova**

pasivní bezpečnost; tramvaj; zranění hlavy; kolize chodce; bezpečnost tramvají; hodnocení.